Investigation on Effects of Aluminum and Magnesium Hypophosphites on Flame Retardancy and Thermal Degradation of Polyamide 6

Qifei Li, Bin Li, Shengqiang Zhang, Mo Lin

Heilongjiang Key Laboratory of Molecular Design and Preparation of Flame Retarded Materials, College of Science, Northeast Forestry University, Harbin 150040, People's Republic of China

Received 10 February 2011; accepted 21 September 2011
DOI 10.1002/app.35678
Published online 17 January 2012 in Wiley Online Library (wileyonlinelibrary.com).

ABSTRACT: Two hypophosphites, aluminum hypophosphite (AlHP) and magnesium hypophosphite (MgHP), were applied to obtain flame retardant polyamide 6 (FR-PA6) composites. UL-94 and limiting oxygen index results indicated that AlHP contributed both good flame retardance and antidripping ability for PA6, while MgHP did not. Based on thermogravimetric analysis (TGA), AlHP and MgHP presented the different thermal degradation behavior. That is, the quick decomposition of AlHP took place at lower temperature than that of MgHP. AlHP promoted the early thermal degradation of PA6 and formed more char residue. The thermal decomposition mechanisms of AlHP and MgHP in nitrogen or air were suggested. Scanning electron microscope and X-ray photoelectron spectroscopy indicated that in the existence of AlHP, the morphological structures of char residue were more homogenous, and compact, and more char residue was formed. These results well illustrated the difference of the flame retardancy between AlHP and MgHP. Mechanical properties of PA6/AlHP and PA6/MgHP were also obtained. © 2012 Wiley Periodicals, Inc. J Appl Polym Sci 125: 1782–1789, 2012

Key words: polyamide 6; aluminum hypophosphite; magnesium hypophosphite; flame retardancy; thermal degradation

INTRODUCTION

Polyamide 6 (PA6) is an important thermoplastic at a wide range of engineering applications, such as electronic and electric (E&E) aspects. However, many applications of PA6 are seriously restricted, due to its inflammability, with a low limiting oxygen index (LOI) value and severe dripping. Therefore, how to improve the flame retardance of PA6 has become an important research topic.[1–4]

To obtain flame retardant PA6 composites, several kinds of flame retardants have been used, including halogen-containing flame retardants and halogen-free flame retardants. The halogen-containing flame retardants are well known to be very effective in PA6, however, due to the release of a quantity of corrosive and toxic gases and black smoke during burning, their applications have been seriously limitted.[5] Therefore, the halogen-free flame retardants have been used to replace halogen containing products due to their environmentally friendly properties.[6] The halogen-free flame retardants for polyamides include metal hydroxides,[6] red phosphorus,[7–9] ammonium polyphosphate,[10,11] melamine polyphosphate (MPP) and melamine cyanurate,[12–18] organic clay, and some organic phosphorus containing compounds.[19–22] Metal hydroxides, such as $Mg(OH)_2$ and $Al(OH)_3$, are environmentally friendly, but due to their low flame retardant efficiency and high addition, mechanical properties of PA6 are destroyed clearly. Red phosphorus is an efficient halogen-free flame retardant, but its application is limited because of its dark color and poisonous phosphine released during the processing. Melamine polyphosphate is considered to be an important and effective flame retardant for the glass fiber reinforced PA composites, but an optimal flame-retardant level is hardly obtained at a low content.[23] Melamine cyanurate is also an important flame retardant for PA6, but it is not effective in glass fiber reinforced PA6. In fact, phosphorus-containing flame retardants are very effective in the flame retardancy of PA6. Previous investigations show that phosphorus element can act in both the condensed and the gas phase. In the gas phase, it results in flame inhibition through radical trapping. In the condensed phase, it promotes the formation of carbon char or inorganic residues. The flame retardant activity of phosphorus-containing flame retardants depends on their chemical structures, polymer structures and the interaction with other additives.[24] Recently, aluminum hypophosphite (AlHP) and aluminum phosphinates (AlPI)

Correspondence to: B. Li (libinzh62@163.com).

have been investigated as a novel class of phosphorous flame retardants for PA. AlPI, MPP, and zinc borate were reported as a very effective flame retardant system for glass fiber reinforced PA66.[24] AlPI vaporizes and acts effectively as a flame inhibitor in the gas phase. The aluminum and boron phosphates enhance the stability of the residue by means of forming a barrier and protect the underlying polymer against the fire. Aluminum phosphinate can promote PA6 to form a char layer so as to stop heat transfer and decrease onset temperature of thermal degradation.[25] AlHP also is a good flame retardant for PA6 and glass fiber reinforced PA6.[26] However, the investigation on its flame retardant mechanism has yet been rarely reported.

In this article, the flame retardancy and thermal degradation of AlHP and magnesium hypophosphite (MgHP) for PA6 were comparatively investigated by means of LOI, UL-94 rating, thermogravimetric analysis (TGA), X-ray photoelectron spectroscopy (XPS), and scanning electron microscopy (SEM).

EXPERIMENTAL

Materials

PA6 used in this work was produced by Harbin Longfei Nylon Engineering Plastics Company. MgHP and AlHP (industrial grade) were offered by Jinyuan Chemical.

Sample preparation

The PA6 composites were prepared by the melt blending process in a twin-screw extruder. The temperature of the extruder was set as 210, 230, 230, 235, 230, and 210°C from feed end to die end, respectively. The loading of hypophosphites in PA6 composites is fixed at 18, 20, 24, and 28 wt %, respectively.

Thermogravimetry analysis tests

TGA experiments were performed using PerkinElmer Pyris 1 Thermal Analyzer with a pure nitrogen or air flow of 30 mL min^{-1}. The samples were heated in platinum pans from 50 to 700°C at a heating rate of 10°C min^{-1}. The weight of the samples was kept within 1.5–4 mg. All thermal degradation data were obtained from TG and DTG curves.

Differential scanning calorimetry tests

Differential scanning calorimetry (DSC) tests were carried out on PerkinElmer Diamond DSC. The weight of each sample was ranged from 2 to 5 mg. All samples were heated from 50 to 450°C at a heating rate of 10°C min^{-1}. All endothermic and exothermic data were obtained from DSC curves.

Flame retardancy tests

The flame retardancy of the composites was determined using the UL 94 classification according to IEC 60695-11-10 and the LOI according to ISO4589-1984. LOI data of all samples were obtained at room temperature on an oxygen index instrument (JF-3) produced by Jiangning Analysis Instrument Factory. The dimensions of all samples are 130 × 6.5 × 3.2 mm^3.

Vertical burning rates of all samples were carried out on a CZF-2 instrument produced by Jiangning Analysis Instrument Factory. The sample dimensions are 125 × 12.5 × 3.2 and 125 × 12.5 × 1.6 mm^3, respectively, according to UL-94 standard. UL-94 test results are classified by burning ratings V-0, V-1, or V-2.

Mechanical properties tests

Determination of tensile strength of all samples was performed by Regeer computer controlled mechanical instrument (Shenzhen Regeer Instrument) according to ASTM D638. Determination of Izod impact of all samples was performed by notched izod impact instrument (Chengde Precision Instrument) according to ASTM D256.

Scanning electron microscopy

SEM was used to examine the morphology of the char residue obtained from the vertical burning tests using a FEI QuanTa200 SEM. The accelerating voltage was 15 kV. The samples were coated with a thin layer of gold by sputtering before the SEM imaging.

X-ray photoelectron spectroscopy

XPS analysis was carried out in an ultrahigh vacuum system equipped with a K-alpha hemispherical electron analyzer (Thermofisher Scienticfic), using a monochromated Al K_α source, at a base pressure of 1.0×10^{-8} mbar. C, N, P, O, and Al or Mg elements were analyzed.

RESULTS AND DISCUSSION

Flame retardancy

AlHP and MgHP were used in PA6 to obtain flame retardant polyamide 6 (FR-PA6) composites including PA6/AlHP and PA6/MgHP. Table I gives the effect of AlHP and MgHP on the flame retardancy of FR-PA6 composites, based on LOI and vertical burning rating (UL-94) tests.

TABLE I
The Flame Retardancy of FR-PA6 Composites

Samples	Components (%)		Flame retardancy		
	PA6	FR	LOI (%)	UL-94 (3.2 mm)	UL-94 (1.6 mm)
PA6	100	0	21.0	Burning	Burning
PA6/AlHP	82	18	25.0	V-0	V-2
	80	20	25.6	V-0	V-2
	76	24	25.6	V-0	V-0
	72	28	26.8	V-0	V-0
PA6/MgHP	82	18	22.5	Burning	Burning
	80	20	22.5	Burning	Burning
	76	24	22.5	V-2	Burning
	72	28	23.0	V-2	V-2
	70	30	23.0	V-2	V-2

From LOI data shown in Table I, PA6 is a flammable polymer, accompanied by melt dripping, and its LOI value is only 21%. When the loading of AlHP in PA6 was 18 wt %, LOI value of the PA6/AlHP composite increased to 25%, and with the increase of AlHP, the LOI values of PA6/AlHP composites slowly increased. When the addition of AlHP was 28 wt %, its LOI value reached 26.8%. Based on the vertical burning results in Table I, all the PA6/AlHP samples with 3.2 mm thickness passed UL-94 V-0 rating. When the addition of AlHP was more than 24 wt %, the PA6/AlHP with 1.6 mm thickness passed UL-94 V-0 rating. For PA6/MgHP composite systems, when the addition of MgHP in FR-PA6 was 18 or 20 wt %, LOI value of the PA6/MgHP was only 22.5, compared to pure PA6, the LOI value only increased 1.5. When the addition of MgHP was 24, 28, and 30 wt %, LOI value of PA6/MgHP composites was 22.5, 23, and 23, respectively. Their vertical burning rating only reached UL-94 V-2 (3.2 mm). It is a very interesting result obtained from above that AlHP showed higher flame retardant efficiency in PA6 than MgHP, despite a close phosphorus content in both AlHP (41.9 wt %) and MgHP (40.3 wt %).

Thermal degradation behavior

To understand the difference of flame retardancy between AlHP and MgHP, the thermal degradation behavior of two hypophosphites, pure PA6 and FR-PA6 composites with 24 wt % hypophosphites, was carried out in nitrogen and air.

Figure 1 gives the TG curves of AlHP and MgHP in nitrogen gas and air. Table II gives their TG data in nitrogen gas and air. From Figure 1(a), it was found that the thermal degradation behavior of AlHP in nitrogen gas showed at two stages. In the first stage, the weight loss of AlHP was 23 wt %, the thermal degradation peak appeared at 363°C, and the maximum thermal degradation rate (R_{peak}) was 14.6% min^{-1}. In the second stage, the weight loss was 6.6 wt %, the thermal degradation peak appeared at 458°C, and the maximum thermal degradation rate (R_{peak}) was 1.1% min^{-1}. The residue of AlHP was 71.6 wt % at 700°C. From DSC data in Table III, AlHP showed an endothermic peak (ΔH = 518.8 J g^{-1}) at 348°C, which mainly took place at the first degradation stage of AlHP. Based on TG and DSC data of AlHP, its thermal degradation mechanism in nitrogen was suggested in Scheme 1. The first thermal degradation stage was attributed to

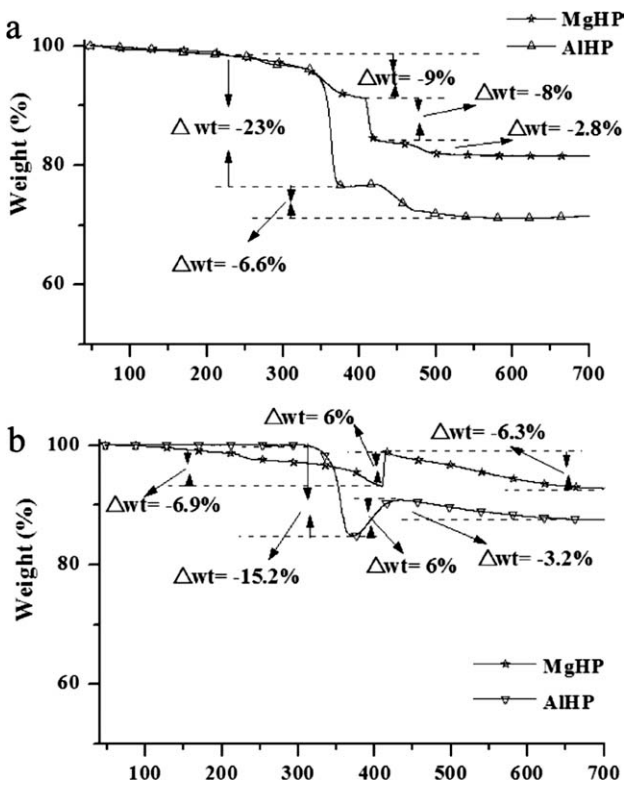

Figure 1 TGA and DTG curves of hypophosphite in (a) nitrogen gas and (b) air.

TABLE II
Thermal Degradation Data of Samples in Nitrogen and Air by TG

	Samples	$T_{initial}$ (°C)	R_{1peak}/T_{1peak} (% min^{-1}°C)	R_{2peak}/T_{2peak} (% min^{-1}°C)	R_{3peak}/T_{3peak} (% min^{-1}°C)	Char residue (%), 700°C
In nitrogen	AlHP	261	−14.6/363	−1.1/458		71.6
	MgHP	252	−1.3/356	−10.2/411	−0.7/479	81.5
	PA6	374	−24.5/441	–	–	5.8
	PA6/AlHP	334	−13.7/396	–	–	26.0
	PA6/MgHP	358	−16.6/416	–	–	23.7
In air	AlHP	337	−9.9/335	1.8/394	–	87.6
	MgHP	229	−1.1/222	57.6/411	–	92.8
	PA6	307	−20.3/427	−2.2/550	–	0
	PA6/AlHP	260	−7.2/386	−0.9/599	–	23.3
	PA6/MgHP	351	−12.1/423	−1.3/557	–	23.7

the reaction that AlHP decomposites to produce phosphine and aluminum hydrogen phosphate and absorb heat, and the second stage is due to the condensation of aluminum hydrogen phosphate. This result is in agreement with the reported one.[27] For MgHP in nitrogen gas, three stages appeared in the thermal degradation process of MgHP. In the first stage, the weight loss of MgHP was 9 wt %, and the thermal degradation peak appeared at 356°C and the maximum thermal degradation rate (R_{peak}) was 1.3% min^{-1}. In the second stage, the weight loss was 8 wt %, and the thermal degradation peak appeared at 411°C and the maximum thermal degradation rate (R_{peak}) was 10.2% min^{-1}. In the third stage, the weight loss was 2.8 wt %, and the thermal degradation peak appeared at 479°C and the maximum thermal degradation rate (R_{peak}) was 0.7% min^{-1}. The residue of MgHP was 81.5 wt % at 700°C. Based on DSC data in Table III, MgHP showed two mainly endothermic peaks at 371°C (ΔH = 187.5 J g^{-1}) and 405°C (ΔH = 454.2 J g^{-1}), which, respectively, appeared at the first and second stages. These results indicated that the thermal degradation mechanism of MgHP (see Scheme 2) is different with that of AlHP. MgHP first decomposites to produce phosphine, hydrogen, and phosphite, and then the second stage is attributed to the decomposition reaction of phosphite to produce phosphine and phosphate. Finally, acidic phosphate dehydrates to the condensation phosphate.[27]

Their thermal degradation behavior in air is much different with one in nitrogen gas. From Figure 1(b), the thermal degradation of AlHP in air showed three stages, which are the weight loss stage (320–360°C), the weight increase stage (360–420°C) and the weight slight loss stage (>420°C), respectively. Meanwhile the thermal degradation of MgHP also showed three stages, that is, the weight loss stage (220–400°C), the weight sharp increase stage (400–420°C) and the weight slight loss stage (>420°C). From Table III, in air AlHP presented an exothermic peak before 380°C (ΔH = 820.2 J g^{-1}), and in air MgHP showed three exothermic peaks at 370, 380 ($\Delta H_1 + \Delta H_2$ = 278.6 J g^{-1}), and 396°C (ΔH_3 = 601.3 J g^{-1}).

Under air condition, their thermal degradation mechanisms were suggested in Schemes 3 and 4. For AlHP, the exothermic peak is attributed to the oxiditive reactions of phosphine, whereas three exothermic peaks of MgHP are attributed to the oxiditive reactions of phosphine and hydrogen. The weight increase stage was due to the oxidation of hypophosphite and phosphite in the condensed phase, and the weight loss in the third stage is attributed to the condensation of acidic phosphate. Phosphine is considered as a radical scavenger that inhibits radicals transfer in flame zone. Hydrogen produced could produce hydrogen radicals, resulting in easy flammability of the composites.[27]

From Figure 2(a), it was found that the thermal degradation behavior of PA6 presented only one peak of decomposition at 441°C, and the thermal degradation rate (R_{peak}) was very fast (24.5% min^{-1}), the char residue of PA6 was 5.8 wt % at 700°C. When 24 wt % AlHP was added, the thermal

TABLE III
The DSC Data of Samples in Nitrogen Gas and Air

	Endothermic peak (in nitrogen)				Exothermic peak (in air)					
Samples	T_{1peak} (°C)	ΔH_1 (J/g)	T_{2peak} (°C)	ΔH_2 (J/g)	T_{1peak} (°C)	ΔH_1 (J/g)	T_{2peak} (°C)	$\Delta H_2 + \Delta H_1$ (J/g)	T_{3peak} (°C)	ΔH_3 (J/g)
AlHP	348	518.8	–	–	353	820.2	–	–	–	–
MgHP	371	187.5	405	454.2	370	–	381	278.6	396	601.3

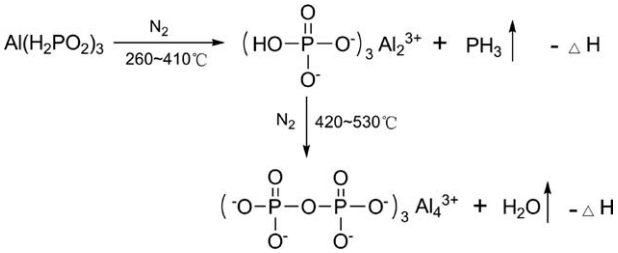

Scheme 1 The thermal degradation mechanism of AlHP in nitrogen.

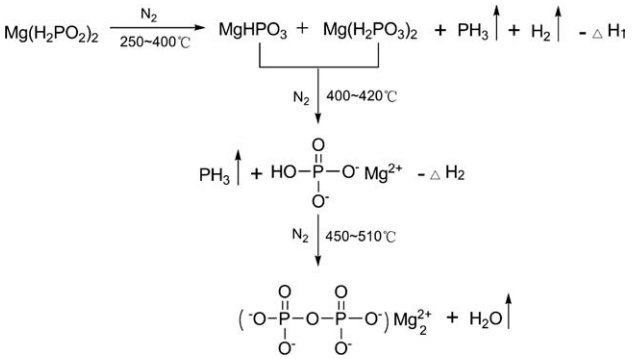

Scheme 2 The thermal degradation mechanism of MgHP in nitrogen.

stability and the decomposition behavior of PA6 were changed. The T_{peak} and R_{peak} of PA6/AlHP were 396°C and 13.7% min^{-1}, respectively, and the char residue of PA6/AlHP was 26.0 wt % at 700°C. When 24 wt % MgHP was added, the T_{peak} and R_{peak} of PA6/MgHP were about 416°C, 16.6% min^{-1}. AlHP could promote PA6 to degrade earlier and reduce the thermal degradation rate of PA6 more effectively than MgHP. This was because AlHP presented lower thermal degradation temperature than MgHP, acidic phosphate produced presents the better function of catalytic degradation and char formation for PA6.[23] This was beneficial to obtain good flame retardancy of PA6.

Figure 2(b) and Table II show TG curves and data of PA6 and FR-PA6 composites in air. It was found that AlHP and MgHP had more complex decomposition behavior in air than that in nitrogen. The thermal decomposition of neat PA6 showed two degradation steps with T_{peak} at 427 and 550°C in air, while a single degradation step in nitrogen. The second degradation step was attributed to the further decomposition and charring of the remnant PA6 matrix. Under air condition, the thermal degradation behavior of PA6/AlHP and PA6/MgHP was similar as one under nitrogen. However, their thermal degradation rate declined. This result was probably attributed to the inhibiting effect of P-containing radicals on the radical degradation of PA6. P-containing radicals were considered to be produced by the reaction P—H bond with oxygen.

Morphological structures and elements analysis of char residues

Figure 3 shows photographs of the bars of PA6/AlHP and PA6/MgHP composites after the vertical burning test. It was observed that PA6/MgHP composite presented a heavy dripping, whereas PA6/AlHP composite showed the antidripping effect. PA6/AlHP can form a good char residue to protect inner materials and prevent melt dripping from taking place.

Figure 4 shows SEM micrographs of the char residues of FR-PA6 composites with 24 wt % loading of hypophosphites, which were collected from the LOI experiment. The morphological structure of the char residue containing aluminum was more homogenous and compact than the one containing magnesium. There are many crevasses and holes on the surface of char residue containing magnesium. Therefore, during burning, heat and flammable volatiles could easily penetrate the char layer into the flame zone. Because of the good surface morphological structure of the char residue, on the contrary, the char residue surface containing aluminum may effectively stop the transfer of heat and flammable volatiles, resulting in good flame retardancy.

To further understand the char formation ability of hypophosphite containing PA 6 composites, XPS was used to analyze the element composition on the

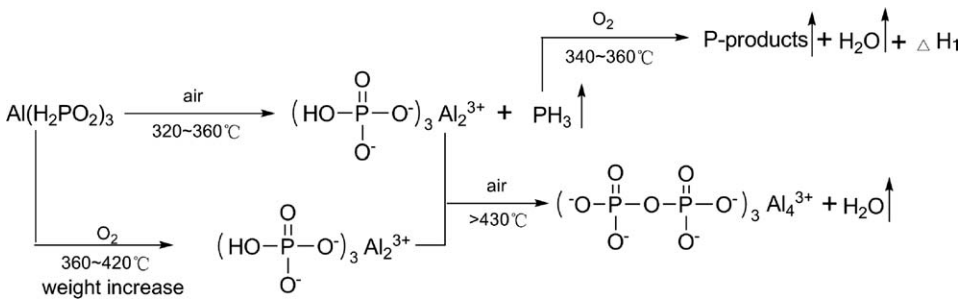

Scheme 3 The thermal degradation mechanism of AlHP in air.

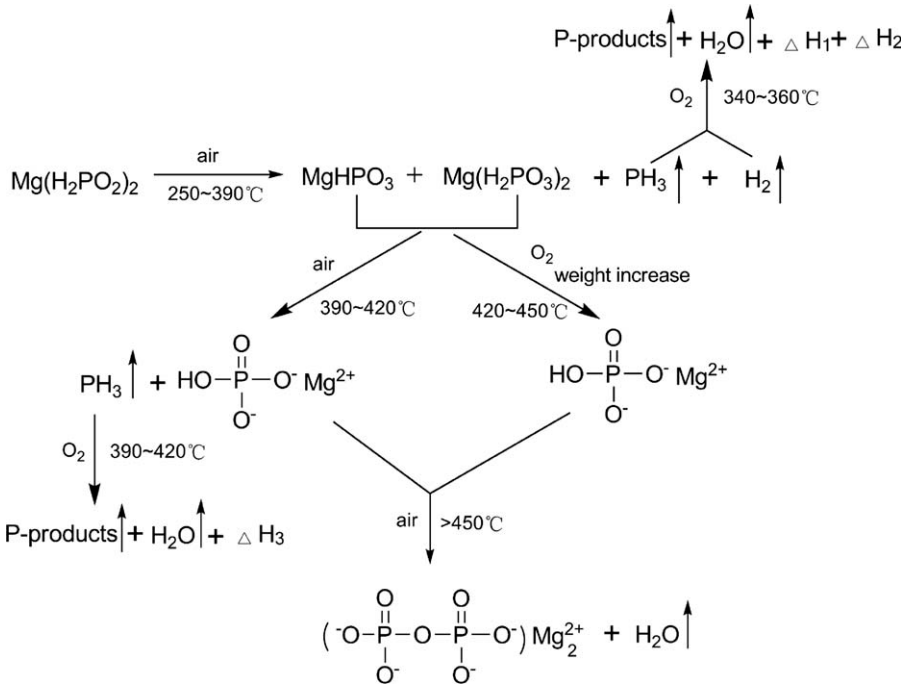

Scheme 4 The thermal degradation mechanism of MgHP in air.

char residue surface. Table IV gives XPS element analysis data of char residues of PA6/AlHP and PA6/MgHP. The char residue mainly consisted of C, O, P, N, and Al (or Mg) elements. From Table IV, the relative atomic percentage of C1s, O1s, and P2p are 68.6, 17.6, and 6.2% for the char residue of PA6/AlHP, respectively, whereas 64.4, 16.7, and 5.8% for the char residue of PA6/MgHP, respectively. The carbon content on the char residue surface of PA6/AlHP was obviously higher than that of PA6/MgHP. This result also indicates that AlHP can

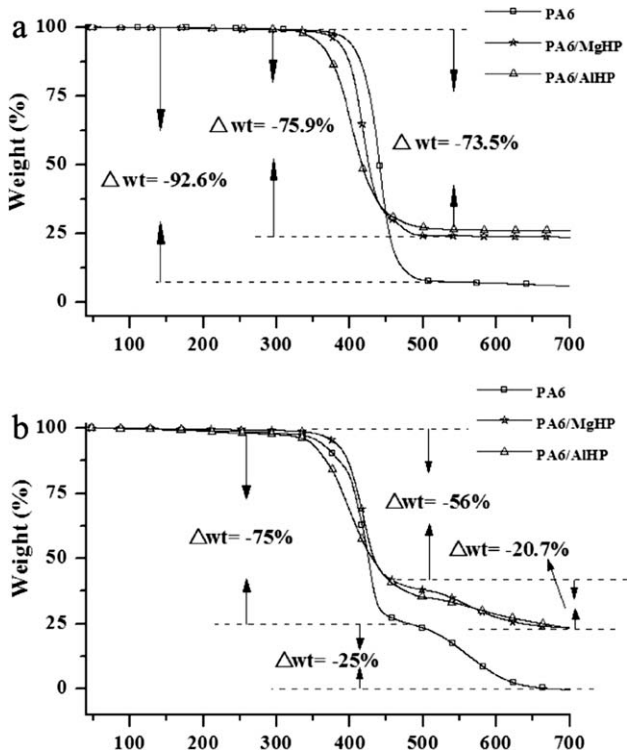

Figure 2 TGA and DTG curves of PA6 and FR-PA6 in (a) nitrogen gas and (b) air.

Figure 3 Photograph of the FR-PA6 bars from UL-94 tests. (a) PA6/MgHP; (b) PA6/AlHP. [Color figure can be viewed in the online issue, which is available at wileyonlinelibrary.com.]

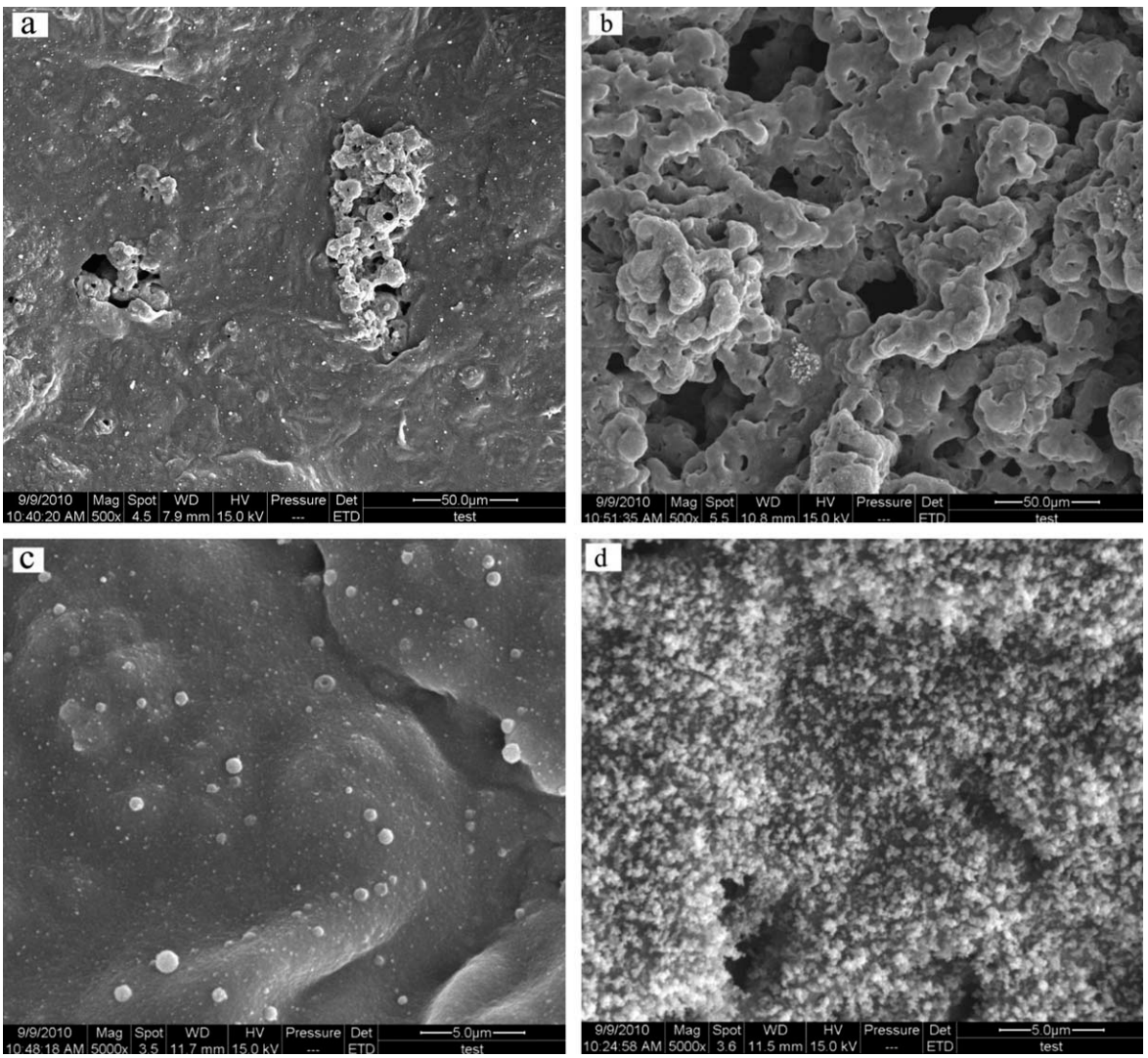

Figure 4 SEM micrographs of the char residues of FR-PA6 from LOI test. (a) PA6/AlHP system ×500; (b) PA6/MgHP ×500; (c) PA6/AlHP ×5000; (d) PA6/MgHP ×5000.

effectively promote the char formation of PA6 during burning, which has been confirmed by SEM results.

Mechanical properties

Figures 5 and 6 give the effect of AlHP and MgHP loading on tensile strength and notched izod impact

TABLE IV
Element Components by XPS Analysis

	PA6/AlHP		PA6/MgHP	
Elements	Peak BE (ev)	Atomic percentage (%)	Peak BE (ev)	Atomic percentage (%)
C1s	283.8	68.6	284.3	64.4
P2p	133.9	6.2	133.0	5.8
O1s	531.9	17.6	530.4	16.7
N1s	399.3	5.3	399.2	9.8
Metal2p	75.0	2.3 (Al)	49.9	3.3 (Mg)

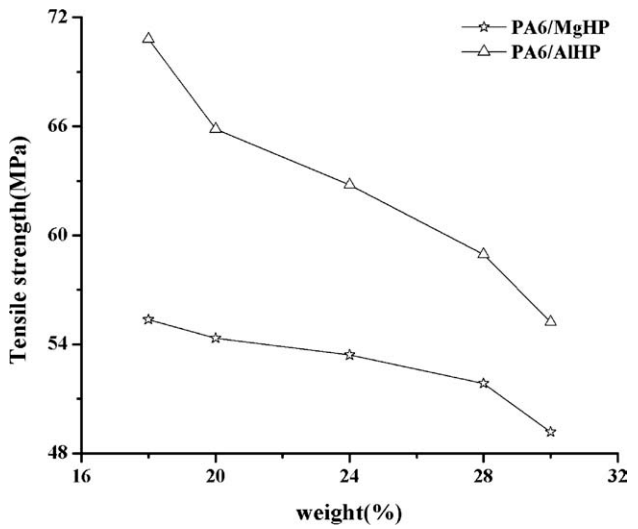

Figure 5 Effect of hypophosphites on tensile strength of FR-PA6.

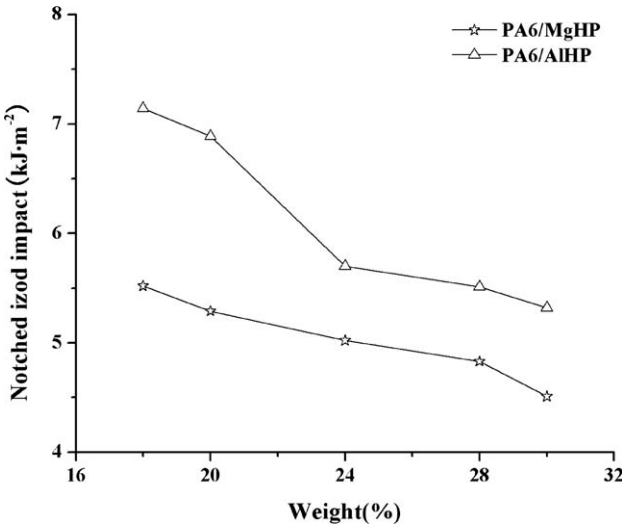

Figure 6 Effect of hypophosphites on notched izod impact of FR-PA6.

of FR-PA6 composites, respectively. The tensile strength and notched izod impact of pure PA6 was 70.4 MPa and 7.0 kJ m^{-2}, respectively. With the increase of AlHP and MgHP loading, tensile strength, and notched izod impact of FR-PA6 composites gradually decreased. In comparison of PA6/AlHP and PA6/MgHP, the tensile strength and notched izod impact of PA6/AlHP were much better than these of PA6/MgHP. These results are probably attributed to the complex ability of Al^{3+} with N or O atom in PA6 was better than that of Mg^{2+}.

CONCLUSIONS

Flame retardant PA6 composites have been obtained used AlHP and MgHP as halogen-free flame retardants. AlHP presented better flame retardancy in PA6 than MgHP based on LOI values and UL-94 ratings. These different results were attributed to the different thermal degradation of AlHP and MgHP in nitrogen or in air. The former produced phoshine, which was easily oxidized, the later produced phosphine and hydrogen, which were also easily oxidized. On the other hand, AlHP promoted the thermal degradation of PA6 to take place earlier than MgHP. SEM and XPS results proved that AlHP presented the good flame retardancy and charring ability in PA6. Mechanical properties of PA6/AlHP showed higher than those of PA6/MgHP.

References

1. Casu, A.; Camino, G. M.; Giorgi, De; Flath, D.; Morone, V.; Zenoni, R. Polym Degrad Stab 1997, 58, 297.
2. Jang, B. N.; Wilkie, C. A. Polymer 2005, 46, 3264.
3. Lu, S. Y.; Hamerton, I.; Prog Polym Sci 2002, 27, 1661.
4. Levchik, S. V.; Well, E. D.; Lewin, M. Polym Int 1999, 48, 532.
5. Bras, M. L.; Bourbigot, S.; Félix, E.; Pouille, F.; Siat, C.; Traisnel, M. Polymer 2000, 41, 5283.
6. Fei, G. X.; Liu, Y.; Wang, Q. Polym Degrad Stab 2008, 93, 1351.
7. Balabanovich, A. I.; Levchik, G. F.; Levchik, S. V.; Schnabel, W. Fire Mater 2001, 25, 179.
8. Liu, Y.; Wang, Q. Polym Eng Sci 2006, 46, 1548.
9. Jou, W. S.; Chen, K. N.; Chao, D. Y.; Lin, C. Y.; Yeh, J. T. Polym Degrad Stab 2001, 74, 239.
10. Dahiya, J. B.; Muller-Hagedron, M.; Bockhorn, H.; Kandola, B. K. Polym Degrad Stab 2008, 93, 2038.
11. Riva, A.; Camino, G.; Fomperie, L.; Amigouët, P. Polym Degrad Stab 2003, 82, 341.
12. Gijsman, P.; Steenbakkers, R.; Fürst, C.; Kersjes, J. Polym Degrad Stab 2002, 78, 219.
13. Wu, Z. Y.; Xu, W.; Xia, J. K.; Liu, Y. C.; Wu, Q. X.; Xu, W. J. Chin Chem Lett 2008, 19, 241.
14. Yang, H. C.; Yang, Q.; He, Q. L. Polym Degrad Stab 2009, 94, 1023.
15. Chen, Y.; Wang, Q. Polym Degrad Stab 2006, 91, 2003.
16. Liu, Y.; Wang, Q.; Fei, G. X.; Chen, Y. H. J Appl Polym Sci 2006, 102, 1773.
17. Chen, Y. H.; Wang, Q.; Yan, W.; Tang, T. M. Polym Degrad Stab 2006, 91, 2632.
18. Jahromi, S.; Gabriëlse, W.; Braam, A. Polymer 2003, 44, 25.
19. Dong, W. F.; Zhang, X. H.; Liu, Y. Q.; Gui, H.; Wang, Q. G.; Gao, J. M.; Song, Z. H.; Lai, J. M.; Huang, F.; Qiao, J. L. Eur Polym J 2006, 42, 2515.
20. Lim, S. H.; Dasari, A.; Wang, G. T.; Yu, Z. Z.; Mai, Y. W.; Yuan, Q.; Liu, S. L.; Yong, M. S. Compos B 2010, 41, 67.
21. Cai, Y. B.; Wu, N.; Wei, Q. F.; Zhang, K.; Xu, Q. X.; Gao, W. D.; Song, L.; Hu, Y. Surf Coat Technol 2008, 203, 264.
22. Dong, W. F.; Zhang, X. H.; Liu, Y. Q.; Q. Wang, G.; Gui, H.; Gao, J. M.; Song, Z. H; Lai, J. M.; Huang, F.; Qiao, J. L. Polymer 2006, 47, 6874.
23. Zhao, B.; Hu, Z.; Chen, L.; Liu, Y.; Wang, Y. Z. J Appl Polym Sci 2011, 119, 2379.
24. Branu, U.; Schartel, B.; Fichera, M. A.; Jäger, C. Polym Degrad Stab 2007, 92, 1528.
25. Ramani, A.; Hagen, M.; Hereid, J.; Zhang, J. P.; Delichatsios, M. Fire Mater 2010, 34, 77.
26. Kostangs, S. Chin. Pat. 200480042289.8, 2004.
27. Perry, D. L. Hand book of Inorganic Compounds; CRC Press: New York, 1995.